Environmental Science & Technology

pubs.acs.org/est

Article

Mobilization, Methylation, and Demethylation of Mercury in a Paddy Soil Under Systematic Redox Changes

Jianxu Wang, Sabry M. Shaheen, Min Jing, Christopher W. N. Anderson, Ann-Christin Swertz, Shan-Li Wang, Xinbin Feng, and Jörg Rinklebe*

Cite This: *Environ. Sci. Technol.* 2021, 55, 10133−10141

Read Online

ACCESS | Metrics & More | Article Recommendations | Supporting Information

ABSTRACT: Methylmercury (MeHg) contamination in paddy fields is a significant environmental issue globally since over half of the population of our planet consumes rice. MeHg is a neurotoxin produced by microorganisms in oxygen-limited environments. Microbial effect on MeHg production is a hotspot of research; however, it has been largely ignored how the oxidation−reduction potential (E_h) shapes MeHg formation. Here, we elucidated Hg (de)-methylation in a contaminated soil by increasing E_h stepwise from −300 to +300 mV using a sophisticated biogeochemical microcosm. At the E_h range from −300 to −100 mV, high MeHg concentration and dissolved total Hg (THg) concentration were found due to a high relative abundance of Hg-methylation bacteria (e.g., *Desulfitobacterium* spp.), acidification, and reductive dissolution of Fe(oxyhydr)oxides. At the E_h range from 0 to +200 mV, the formation of colloids leads to adsorption of Hg and as a result colloidal Hg increased. MeHg reduction with E_h (−300 to +200 mV) increase was mainly attributed to a reduced Hg methylation, as dissolved THg and relative abundance of *Desulfitobacterium* spp. decreased by 50 and 96%, respectively, at E_h of +200 mV as compared to E_h of −300 mV. Mercury demethylation might be less important since the relative abundance of demethylation bacteria (*Clostridium* spp.) also decreased over 93% at E_h of +200 mV. These new results are crucial for predicting Hg risks in paddy fields.

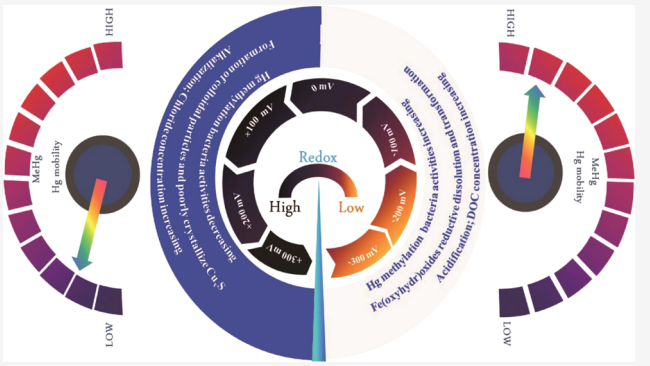

KEYWORDS: *mercury redox chemistry, risk management, Hg (de-)methylation process, biogeochemical cycle*

INTRODUCTION

Geogenic and anthropogenic soil contamination by mercury (Hg) has a global significance.[1,2] More than thousands of hotspots of Hg contamination occur in nonferrous metal (e.g., mercury, gold, lead, and zinc) mining and processing sites and industrial sites worldwide (Figure 1a).[3,4] The dispersion of Hg via solid wastes, liquid wastes, and gas from those hotspots has caused global soil contamination, particularly in farmlands. For instance, a recent national-wide soil surgery conducted by the Chinese government showed that over 1.9% of the collected soil samples are contaminated with Hg.[5] Concerns about global soil Hg contamination have been rapidly increasing because the transformation of Hg into toxic and bioaccumulative methylHg and its accumulation in crops have threatened the health of millions of people in the world.

The bioaccumulation of methylHg in the terrestrial food web via paddy fields is an emerging environmental issue globally, particularly in Asia, where nearly 89% of the world's paddy fields are located (Figure S1). The predication of the biogeochemical behavior of MeHg is essential for the mitigation of MeHg from paddy soils; however, this is challenged by the frequent change in redox potential (E_h) of paddy soil caused by flood−dry cycles, as both microbial and biogeochemical effects on mobilization and (de)-methylation of Hg at specific redox conditions remained unknown.

MeHg formation is a microbially mediated process,[8,9] and bacteria processing the hgcA gene sequence is closely related to Hg methylation.[10] A number of studies demonstrated a MeHg production by single isolated bacteria in the presence of dissolved organic carbon (DOC) and thiols.[11,12] It has been largely ignored how the degree of oxidation−reduction potential (E_h) affects the process of MeHg formation. Rising redox potential reduces Hg bioavailability and MeHg in both soils and sediments.[13,14] However, clear and direct evidence on how E_h fluctuation and E_h-dependent change in biogeochemical processes affect Hg and MeHg is missing to date. The mechanistic understanding of E_h-regulated Hg mobilization

Received: October 29, 2020
Revised: April 9, 2021
Accepted: June 21, 2021
Published: July 2, 2021

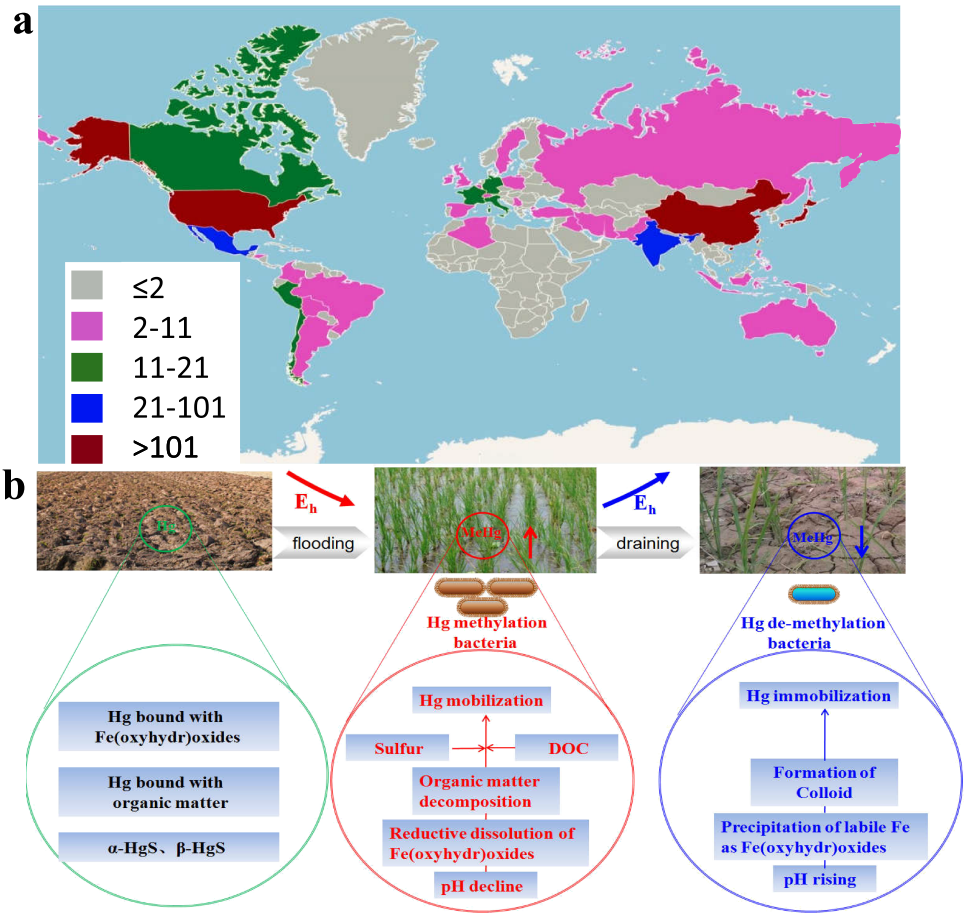

Figure 1. (a) Number of Hg-contaminated sites, which were recorded in the USGS database[6] and published in the literature,[7] in different countries of the world. Different colors of legend indicate that the numbers of contaminated sites in different countries are different. We defined nonferrous metal (e.g., mercury, gold, lead, and zinc) mining and processing sites and industrial sites (e.g., chemicals, etc.) as Hg-polluted sites. The number of Hg-polluted sites was collected from the USGS database and the published literature. (b) Hypothesized model describing the biogeochemical factors participating in MeHg formation during the redox potential (E_h) decreasing and increasing.

and (de)-methylation is fragmented, as the change in Hg-methylation microbial community, the dynamic of carbon and Fe(oxyhydr)oxides and sulfur chemistry and their coupling with Hg mobilization/methylation, with fluctuation of E_h remains to be addressed.

We developed a conceptual model to describe the redox-dependent Hg mobilization and (de)-methylation in soils (Figure 1b). Part 1: Under reducing conditions, the activities of Hg-methylation bacteria (e.g., *Desulfitobacterium* spp.) may increase; anaerobic bacteria use organic matter as the energy source and Fe^{3+} and SO_4^{2-} as electron acceptors,[15] resulting in decomposition of organic matter, dissolution of Fe(oxyhydr)-oxides, and reduction of SO_4^{2-} to S^{2-} and HS^-.[16,17] Thus, Hg associated with Fe(oxyhydr)oxides and organic matter may be liberated. The alteration of organic matter, sulfur, and chloride chemistry may affect the availability of Hg for microbial methylation. For instance, the presence of DOC, sulfide, and Hg^{2+} forms neutrally charged complexes $Hg(SH)_2^0$[18] and HgS^0,[19] which are bioavailable for methylation. The binding of Hg with Cl forms the Hg−Cl bond, which is resistant to methylation. Part 2: Under oxidizing conditions, pH increase and the decreased abundance and activities of Hg-methylation bacteria may diminish MeHg production; ferrous-ion oxidation forms amorphous Fe(oxyhydr)oxides, which can absorb and/or occlude Hg via forming ternary surface complexes.[20,21] The oxidation of sulfide complexes (e.g., FeS_2 and CuS)[22,23] enhances the mobilization of their associated Hg complexes. Colloids formed by precipitation and aggregation of amorphous Fe(oxyhydr)oxides, $CaSO_4$, and salts will adsorb/coprecipitate with Hg.

Here, we used an automated biogeochemical microcosm system, which enables a precise, systematic, and mechanistic control of E_h. This allows one to study the effects of stepwise E_h fluctuation from strong reducing (−300 mV) to oxidizing conditions (+300 mV) on Hg mobilization and (de)-methylation in a contaminated soil, revealing the underlying biogeochemical mechanisms using a combination of geochemical, microbial, and spectroscopic approaches. We particularly addressed the (1) E_h-dependent alteration of dissolved total Hg (THg), colloidal THg, dissolved MeHg, and colloidal MeHg; (2) shift of relative abundance of Hg methylation and demethylation bacteria along E_h fluctuations; (3) dissolution and precipitation of Fe(oxyhydr)oxides during E_h fluctuations, and the impact of these changes on Hg mobilization; and (4) dynamics of colloids, dissolved organic carbon (DOC), Cl^-, and sulfate and their combined effects on Hg mobilization and methylation. The gained knowledge is essential for improving our ability to predict Hg hazards and mitigate its risks in soils and waterlogged sediments at contaminated sites around the world.

https://doi.org/10.1021/acs.est.0c07321
Environ. Sci. Technol. 2021, 55, 10133−10141

MATERIALS AND METHODS

Soil Sample Collection and Characterization. The studied soil was collected from a contaminated paddy field in southwest China (25°63′37.20″N; 105°20′37.40″E). About 200 kg of surface soil samples (0−20 cm in depth) was randomly collected from a 100 m^2 field, transported to the laboratory, air-dried, mixed, and thereafter passed through a 4 mm nylon sieve. The pH, electrical conductivity (EC), organic matter content, mineralogical composition, and particle size distribution of the soil were measured using standard methods[24] (Supporting Information, S1.1). Dilute acid (nitric acid and sulfuric acid (60/40 wt %) at pH 4.2) was used to extract potentially mobile Hg from the soil. The pH and EC of the soil were 8.6 ± 0.08 and 0.16 dS m^{-1}, respectively, and the organic matter content was 1.21%. Total concentrations of Hg and Fe in the soil were 8.9 ± 2.0 mg kg^{-1} and 54.8 ± 0.92 g kg^{-1}, respectively. The minerals, including quartz, kaolinite, muscovite, calcite, gibbsite, and Fe_2O_3, were identified as dominant in the soil using X-ray diffraction (XRD) (Figure S2).

Redox Experiments Using Advanced Biogeochemical Microcosm Technique. A unique biogeochemical microcosm (MC) system, which enables precise control and presetting of redox changes by an automatic-valve regulation system along with high-temporal resolution monitoring of E_h, pH, and temperature, was exploited to simulate changing environmental conditions. Three fully independent MCs were used as triplicates. Each MC was filled with air-dried soil and water at a mass ratio of 1:8. About 15 g of powdered wheat straw was added to each MC to simulate the farming practice of wheat straw returning to farmlands. In addition, 10 g of glucose was added to each MC to serve as the carbon source for microorganisms to eliminate any C-limitation effect. The experimental details have been described elsewhere.[16,25]

The lowest E_h value (−333 mV) was achieved after 65 h through microbial reduction effects. When E_h reached the lowest value, it gradually increased due to the weakened microbial activities by the depletion of carbon sources. It was impossible to maintain E_h at the lowest value by flushing N_2. Therefore, after this E_h window, E_h was raised sequentially in 100 ± 20 mV increments by flushing with synthetic air (N_2/O_2, 79.5/20.5 vol %) or O_2 and each targeted E_h window was maintained by flushing with those gases automatically for about 48 h. Except at −300 mV, six predefinite E_h windows (−200, −100, 0, +100, +200, and +300 mV) were set and subsequently sampled after 48 h of equilibrium. According to Yu and Rinklebe[25] and Rinklebe et al.,[26] the maintenance of soil for about 48 h at a given E_h window was sufficient to reach the equilibrium of E_h-modeled biogeochemical reactions. Redox potential and pH data of each MC were logged every 10 min during the entire experiment. The E_h values shown here were the predefinite E_h windows.

Sampling and Analyses. About 80 mL of soil suspension was taken from the MCs using a 100 mL syringe. Without contact with ambient air, each sample was immediately moved to an anaerobic glovebox under a 95% N_2/5% H_2 atmosphere (A35 anaerobic workstation, Don Whitley Scientific Limited, the United Kingdom) and transferred into two 50 mL centrifuge tubes. Thereafter, samples were centrifuged at 5000 rpm for 10 min and moved again into the anaerobic glovebox, and the supernatants were filtered through 0.45 and 8 μm pore size Millipore nylon membranes (Whatman, Inc.) to obtain the dissolved and dissolved + colloidal fractions, respectively. In this work, we define the size fractions as follows: less than 0.45 μm filtrate is dissolved;[27] less than 8.0 μm filtrate is colloidal + dissolved; and the 0.45−8.0 μm filtrate as colloid.[28] The sedimentated phases from triplicate MCs for each targeted E_h window were mixed with one composite sample. Each composite was further divided into three subsamples for the analysis of the microbial community composition, Fe speciation, and MeHg. The filtrate (<0.45 μm) was divided into six subsamples for Fe, total Hg, MeHg, DOC, SO_4^{2-}, and Cl^- analyses. The other filtrate (<8 μm) was divided into three subsamples for total Hg, MeHg, and colloidal particle analyses. Subsamples for Fe analysis were acidified to 2% trace-metal-grade HNO_3; subsamples for total Hg and MeHg analyses were acidified to 5% HCl (34−37%, Plasma PURE).

Total Hg in dissolved and colloidal fractions was directly measured by a DMA-80 Hg analyzer (Milestone Srl, Sorisole, Italy), which has a detection limit of 0.01 ng.[29] Concentrations of Fe were analyzed by inductively coupled plasma optical emission spectrometry (ICP-OES) (Ultima 2, Horiba JobinYvon, Unterhaching, Germany). The concentrations of DOC were determined by a C/N analyzer (Analytik Jena, Jena, Germany) and those of SO_4^{2-} and Cl^- via an ion chromatograph (Personal IC 790, Metrohm, Filderstadt, Germany). Colloidal particles (Φ < 8 μm) were collected through ultracentrifugation of 6 mL soil suspensions at 14 000*g* for 60 min (CS150GXII, Hitachi, Ltd., Japan). The colloids collected at E_h values of −300, 0, and 300 mV were analyzed for morphology and chemical compositions using a scanning transmission electron microscope (STEM, Hitachi HD-2700, Hitachi High-Technologies Corp., Tokyo, Japan). As for MeHg analysis, liquid samples were distilled to concentrate MeHg, and soil samples were extracted by $CuSO_4$-methanol. Thereafter, MeHg in the solution and extractant were further subjected to extraction with methylene chloride, back-extraction with water, and ethylation into methylethyl-Hg for analysis by a cold vapor atomic fluorescence spectroscopy (CVAFS) detector (CVAFS, Brooks Rand Instruments) according to the USEPA method 1630.[30] Iron speciation in the precipitated sediments was characterized by Fe K-edge X-ray absorption near-edge structure (XANES) spectroscopy. Analytical details and data-quality control are provided in the Supporting Information, S1.2−S1.5.

Microbial Community Analysis. Total genomic DNA in ∼0.25 g of the bulk soil and the soils collected from the targeted redox window was extracted in triplicate using a Fast DNA Spin kit (MP Bio, Santa Ana) using the producer's protocol. The concentration and purity of the extracted DNA (in 1% agarose gels) were monitored using the NanoDrop One (Thermo Fisher Scientific, MA). Thereafter, the dilution of DNA (to 1 ng mL^{-1}) was done according to the monitoring results. The 16S rRNA genes of V4−V5 distinct regions were amplified using 515F/907R primer pairs with a 12 bp barcode.[31] The detailed syntheses of primers and polymerase chain reactions (PCRs), generation of sequencing libraries, and the sequencing of library are given in the Supporting Information, S1.6. Theusearch software was used for sequences analysis. The same operational taxonomic unit (OTU) is defined if the sequences have a similarity equal to or over 97%. In general, an OTU is considered to likely represent a certain species. Each representative sequence was further processed to

https://doi.org/10.1021/acs.est.0c07321
Environ. Sci. Technol. 2021, 55, 10133−10141

annotate taxonomic information (set the confidence threshold to default to 0.5) using the SILVA database.

Statistical Analysis. The mean and standard deviation were calculated from three replicates. One-way analysis of variance (ANOVA) and the least significant difference (LSD) test or (two-tailed) were used to show the significant differences (confidence interval 95%) in means of data.

RESULTS AND DISCUSSION

Effects of E_h/pH Changes on Hg Mobilization. The measured E_h range was −333 to +306 mV (Figure 2), which

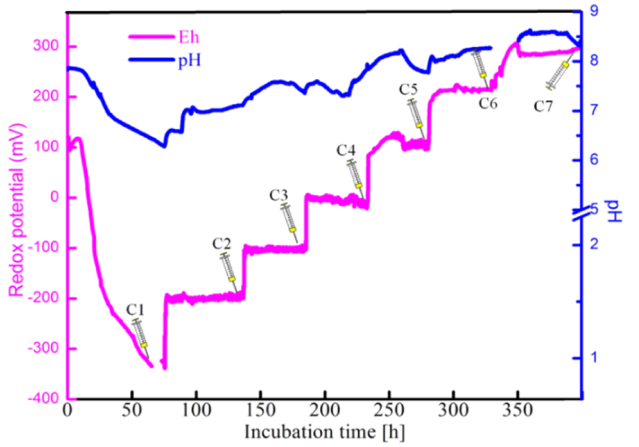

Figure 2. Temporal course of pH-E_h of the soil slurry measured every 10 min under predefinite E_h conditions; C1−C7 indicate that samples were taken at those E_h windows from three individual microcosms.

covers the recorded E_h range of wetland and paddy soils worldwide.[15] The pH showed an E_h-dependent behavior, and it decreased with decreasing E_h and rose again with increasing E_h (Figure 2). The production of CO_2 and organic acids originating from microbial activities and decomposing organic matter might account for the low pH under reducing conditions.[16] The pH of the soil at the start of the experiment (E_h of −300 mV) was 6.2, 2 units lower than the bulk soil (8.2); this acidification might have contributed to Hg mobilization. Potentially mobile Hg, quantified through extraction with dilute acid (pH = 4.2), was 50 ng L^{-1} in the bulk soil, and this sets a maximum limit for Hg mobilization that can be attributed to acidification.

The dissolved total Hg (THg) concentration (483 ng L^{-1}) at E_h of −200 mV was over 8 times higher than Hg mobilized from the bulk soil via the simple dilute acid (pH = 4.2) extraction procedure, inferring that Hg mobilization in the microcosm must be driven by further biogeochemical processes in addition to acidification. The total Hg concentration was greater (483 ng L^{-1}) under reducing than oxidizing conditions (163 ng L^{-1}) (Figure 3A). The dissolved Hg concentration decreased as E_h rose from −300 to +100 mV; however, the Hg concentration increased again as E_h increased from +100 to +300 mV. This redox-dependent variation of dissolved Hg might be a consequence of the integrated effects of biogeochemical alterations of Fe(hydr)-oxides, colloids, and microorganisms.

Effect of Redox Chemistry of Fe(hydr)oxides on Hg Mobilization. The dissolved Fe concentrations (0.81−1.65 mg L^{-1}) were the greatest under reducing conditions (−300 to −200 mV) and decreased sharply to 0.09 mg L^{-1} within the E_h range of −100 to 0 mV (Figure 3B). They decreased further to 0.02 mg L^{-1} as E_h increased from +100 to +300 mV (Figure 3B). A positive correlation between dissolved Fe and Hg was observed (R^2 = 0.37, P < 0.05, Figure S3). Under reducing conditions (acidic), Hg associated with Fe(hydr)oxides together with Fe could be released as a function of reductive/acidic dissolution of Fe(hydr)oxides, while under oxidizing conditions (alkaline), dissolved Fe precipitates as amorphous Fe(hydr)oxides, which might adsorb Hg. Many bacteria of *Bacillus* spp. drive Fe(hydr)oxides reduction,[32] and representative species showed a high relative abundance (Table S1) in our soil (biotic reduction).[33] However, the separation of abiotic and biotic processes is difficult since organic matter is present in the soil[34] and abiotic processes should also be considered. The ferrihydrite proportion decreased by 13% in the soil collected at E_h of −300 mV as compared to the bulk soil, supporting our assumption of reductive dissolution of Fe(hydr)oxides. Further, the increase

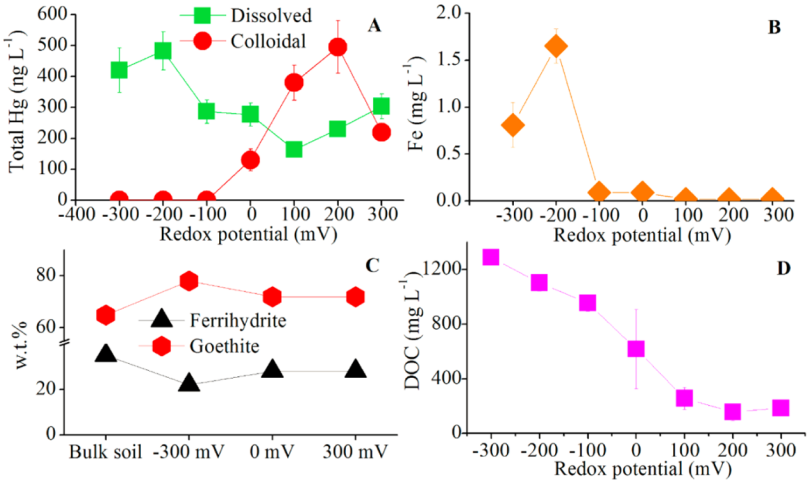

Figure 3. (A) Concentration of Hg in the dissolved and colloidal phases in the soil of each E_h condition. (B) Dissolved Fe concentration in the soil of each E_h condition. (C) Iron (Fe) speciation in the bulk soil and the soils collected at E_h values of −300, 0, and +300 mV. (D) Concentrations of dissolved organic carbon (DOC) in the soil solution of each E_h condition. Error bars in (A), (B), and (D) stand for the standard deviation of the three independent microcosms that served as replicates (n = 3).

https://doi.org/10.1021/acs.est.0c07321
Environ. Sci. Technol. 2021, 55, 10133−10141

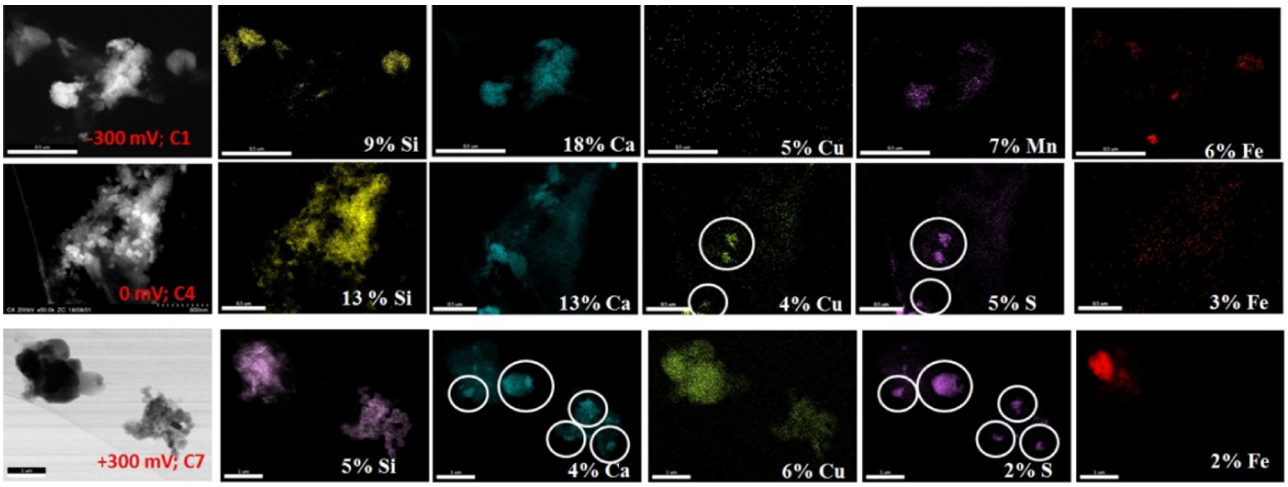

Figure 4. Scanning transmission electron microscope (STEM) images of the colloidal particles (−300, 0, and +300 mV) and STEM−energy-dispersive spectroscopy (EDS) digital images of silicon (Si), calcium (Ca), copper (Cu), manganese (Mn), aluminum (Al), iron (Fe), and sulfur (S) in the particles. The white circles indicate a similar distribution pattern of Cu and S at E_h of 0 mV and of Ca and S at E_h of +300 mV. The STEM images of C, N, O, Mg, Cl, Zn, P, F, Na, and K are shown in Figure S6.

of E_h from −300 to 0 mV led to a 6% increase of ferrihydrite, while further increasing E_h from 0 to +300 mV did not change the Fe speciation. These results might indicate the formation of amorphous Fe(hydr)oxides at E_h over 0 mV (Figures 3C and S4), and these newly formed Fe(hydr)oxides may be associated with Hg adsorption.

Effect of Colloids on Hg Availability. We found a vital role of colloids in Hg immobilization during redox change. Colloidal Hg concentrations (130−495 ng L^{-1}) were higher than dissolved Hg (163−303 ng L^{-1}) at the E_h range from 0 to +300 mV, while the opposite trend was observed at the E_h range from −300 to −100 mV (Figure 3A). The E_h-dependent changes in colloids should explain the geochemical behavior of the colloidal Hg. More colloids were presented in the soil at the E_h range from 0 to +300 mV than from −300 to −100 mV (Figure S5).

The STEM−EDS analysis showed the presence of calcium (18%), silica (9%), Fe (6%), Mn (7%), and Cu (5%) in the colloids collected at E_h of −300 mV (Figure 4). More elements were detected in the colloids collected at E_h values of 0 (Mg, S, Cl, P, K, S, and Zn) and +300 mV (Na, Mg, Al, and K) as compared to −300 mV (Figures 4 and S6). The similar distribution pattern of Ca and O in the colloids at all E_h ranges demonstrates the common presence of carbonates (e.g., calcite), which is in line with the XRD result of the bulk soil (Figure S2). A similar distribution pattern of Cu and S and of Ca and S in the colloids collected at E_h values of 0 and +300 mV, respectively, indicates the presence of Cu_xS[35] and $CaSO_4$ (e.g., gypsum and anhydrite) (Figure 4). Carbonate, Cu_xS, and Fe oxides were able to absorb Hg.[21,36,37] Also, Hg could coprecipitate with $CaSO_4$.[38] These immobilization processes could result in a decrease of dissolved Hg and an increase of colloidal Hg concentration.[39,40]

Effect of Sulfate and DOC on Hg (Im)-Mobilization. Concentrations of DOC ranged between 157 mg L^{-1} at E_h of +200 mV and 1288 mg L^{-1} at E_h of −300 mV (Figure 3D). These values were comparable to a previous study that reported that total organic carbon and DOC in soils spiked with straw were 17 700 and 654 mg kg^{-1}, respectively.[41] The DOC concentration was higher at lower E_h, which was likely due to the microbial decomposition of straw and glucose. In other words, microbial activities (e.g., Fe(hydr)oxide reducers) were more active at low E_h, and this would intensify microorganism-associated biogeochemical reactions (e.g., Fe(hydr)oxide reductive dissolution).[42] For instance, the presence of the highest concentrations of DOC, dissolved Fe, and Hg at the lowest E_h demonstrated the stimulated reductive dissolution of Fe(hydr)oxides by a carbon source, releasing Fe, and the associated Hg. The DOC concentration decreased gradually with the increase of E_h, which might be attributed to both the depletion of straw and glucose and adsorption of DOC by newly formed Fe(hydr)oxides.[43,44] DOC can enhance the Hg mobilization by acting as a carrier, as supported by a strong positive correlation between DOC and Hg (R^2 = 0.48, P < 0.05) (Figure S7).

We expected a significant dissimilatory reduction of sulfate under reducing conditions (−300 to −100 mV).[15] However, concentrations of sulfate were higher in the E_h range from −300 to 0 mV than from +100 to +300 mV (Figure S8). This may have been due to poor sulfate reduction reactions in the E_h range from −300 to 0 mV or the scavenging of sulfate from the soil liquid phase at the E_h range from +100 to +300 mV. We propose two scenarios to support this explanation. First, preferential or concurrent reduction of NO_3^- and Fe(hydr)-oxides preserves sulfate since these compounds are more thermodynamically favorable for reduction than sulfate.[15] Second, sulfate reduction at high E_h might be related to newly formed Fe(hydr)oxide adsorption, as proposed by Sparks,[45] who reported that sulfate could be absorbed by Fe(hydr)oxides via the formation of surface outer- and inner-sphere complexes.

Composition of the Microbial Community at Predefinite E_h Windows. Soil microbial community compositions at the genera level differed significantly between the predefinite E_h windows (Figure 5). Among the identified genera (Figure S9), *Clostridium* spp. and *Desulfitobacterium* spp. accounted for 1.4−16 and 0.15−1.57% of abundance of microorganisms across E_h ranges from −300 to 0 mV, respectively, and 0.9−3.1 and 0.03−0.06% for E_h ranges from +100 to +300 mV, respectively (Figure 5). The relative abundances of *Clostridium* spp. and *Desulfitobacterium* spp. significantly decreased as a function of E_h increase (P < 0.05,

https://doi.org/10.1021/acs.est.0c07321
Environ. Sci. Technol. 2021, 55, 10133−10141

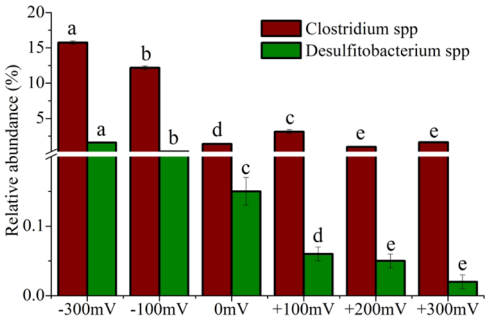

Figure 5. Relative abundances of *Clostridium* spp. (summarization of the relative abundance of *Clostridium_sensu_stricto_1* and *Clostridium_sensu_stricto_12*) and *Desulfitobacterium* spp. in the soil as a function of the redox potential. Error bars are the standard deviation of the three independent replicates (n = 3). The small case letters on the top of each bar indicate if the difference in relative abundance of each genus among different redox conditions is significant at the P < 0.05 level.

ANOVA), but they remained unchanged when E_h increased to +200 mV. The anaerobic habit of *Clostridium* spp. and *Desulfitobacterium* spp. could explain their variation under different redox conditions. Many bacteria in *Desulfitobacterium* spp. (e.g., *Desulfitobacterium metallireducens*, *Desulfitobacterium dehalogenans*) had been identified as Hg methylators,[46] and *Clostridium* spp. were considered as Hg demethylators (*Clostridium_sensu_stricto_1* and *Clostridium_sensu_stricto_12*).[47] The presence of *Desulfitobacterium* spp. and *Clostridium* spp. may closely relate to Hg methylation and demethylation in our soil during redox fluctuations. Results of the microbial community composition on the class level are presented in the Supporting Information, S2.1.

Redox-Dependent Hg Methylation and Demethylation. Dissolved MeHg decreased with the increase in E_h (Figure 6A). Mercury methylation potential (efficiency), defined as the ratio of MeHg to THg, is used to indicate the net MeHg production in sediments or soils.[48,49] This Hg-methylation potential showed a similar trend to the dissolved MeHg and was higher at E_h ranges between −300 and −100 mV (105−123 × 10^{-6}) than within the range between 0 and +300 mV (18−52 × 10^{-6}) (Figure 6B). These results indicate that Hg tends to be methylated under strong reducing conditions. Mercury methylation can occur via the biotic and abiotic pathways.[50−52] Abiotic methylation needs suitable and sufficient methyl donors (e.g., methylcobalamin),[53] components that should be absent under our experimental microcosm conditions as they are usually present inside organisms. We therefore believe that Hg methylation in our soil was dominantly biotic. Among the identified bacteria (genus), *Desulfitobacterium* spp. is a potential Hg methylator (Figure S9). The Hg-methylation potential increased with the increase in the relative abundance of *Desulfitobacterium* spp., which supports the assumption of a strong interaction between bacteria of this genus and Hg methylation (Figure S10A).

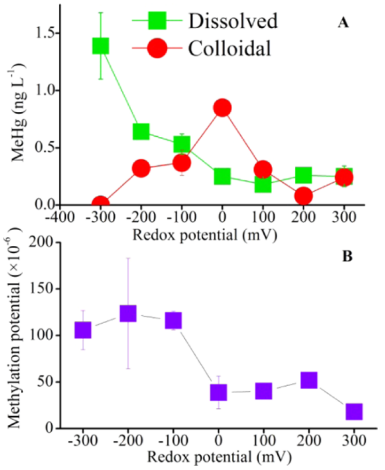

Figure 6. (A) Concentration of MeHg in the dissolved and colloidal phases of soil samples collected at each E_h condition. (B) Methylation potential of soil samples at each E_h condition. The error bars are the standard deviation of the three independent microcosms, which served as replicates (n = 3).

Colloidal MeHg concentration, as a function of E_h, showed a different distribution with the dissolved MeHg (Figure 6A). The colloidal MeHg concentration enhanced as E_h increased from −300 to −100 mV, reaching a maximum at 0 mV, and then reduced again at higher E_h. The increase in colloidal MeHg concentration was accompanied by a decrease in dissolved MeHg concentration at the E_h range from −300 to 0 mV. This led to our hypothesis that the high concentration of colloidal MeHg observed under these E_h ranges might be attributed to the sorption and coprecipitation of MeHg with colloids.[54] However, the underlying mechanism of reduced colloidal MeHg concentration for E_h values >+100 mV might be different. The concentrations of dissolved and colloidal MeHg showed a decreasing trend when E_h values were higher than +100 mV (Figure 6A). For this phenomenon, we propose two scenarios. On one hand, microbially mediated methylation became weak, as dissolved THg concentration and the relative abundance of Hg-methylation bacteria (e.g., *Desulfitobacterium* spp.) decreased with increasing E_h (Figures 3A and 5). On the other hand, MeHg demethylation could promote its concentration reduction. MeHg demethylation occurs through both biotic and abiotic pathways.[55] Biotic demethylation should be linked to *Clostridium_sensu_stricto_1* and *Clostridium_sensu_stricto_12* (0.9−16%) as they were likely to be MeHg demethylators[47] and presented at high relative abundances in the soil during the redox changes (0.9−16%). However, their relative abundances were the highest at E_h of −300 mV at which the highest MeHg concentration was observed (Figure S10B). We attributed this phenomenon to the greater MeHg production rate than its demethylation rate at low E_h. With E_h increasing, particularly over +100 mV, Hg methylation became rather weak, and the MeHg demethylation rate might thus exceed its production rate. Photodecomposition[55]-mediated demethylation is expected to be of minor importance here because the used microcosm system was covered with aluminum foil to avoid the intrusion of light.

Effect of Biogeochemical Factors on Hg Methylation and Demethylation. The mercury methylation potential (ratio of MeHg to THg[56]) was positively correlated with the ratio of DOC to THg and negatively correlated with the chloride concentration (Figures S11 and S12). We interpret this as an integrated effect of Hg mobilization, DOC, and Cl^- on Hg methylation as follows. Increasing the ratio of DOC to dissolved Hg appears to enhance Hg methylation. DOC contains a diverse range of organic carbon components with different molecular weights, functional groups, and polarities, and they have various effects on Hg methylation in the environment. For example, Bravo et al.[57] reported that

https://doi.org/10.1021/acs.est.0c07321
Environ. Sci. Technol. 2021, 55, 10133−10141

phytoplankton-derived organic compounds were more capable of enhancing Hg methylation than terrigenous organic matter in boreal lake sediments due to their difference in chemical composition. We hypothesize that increasing the DOC concentration might increase the abundance of components such as hydrophobic surfaces in the soil,[58] enhancing Hg methylation. The negative correlation between the Cl^- and MeHg-to-THg ratio (Figures S8 and S12) indicates that a high concentration of Cl^- inhibits Hg methylation. This might be attributed to the formation of the Hg−Cl bond, which is more resistant to methylation than the Hg−O bond.[59]

Summary, Highlights, and Environmental Implications. The global reduction of Hg^0 emission is the aim of the Minamata Convention, which entered into force in 2017. However, the risks of MeHg in previously contaminated environments, particularly in waterlogged soils and sediments, cannot be eliminated naturally. The predication of the biogeochemical behavior of MeHg is a prerequisite to minimizing Hg risk to human beings. Here, our results deepen the understanding of the Hg contamination process and its biogeochemical cycle in paddy soils and sediments. We demonstrate that decreasing the O_2 (anaerobic conditions) favored the establishment of Hg-methylation bacteria (*Desulfitobacterium* spp.) and reductive dissolution of Fe-(oxyhydr)oxides, leading to the liberation and methylation of Hg in the soil. During E_h change from anaerobic to aerobic, the gradual decrease of the relative abundance of Hg-methylation bacteria (*Desulfitobacterium* spp.) and dissolved Hg concentration resulted in a reduction of MeHg. The reduction of dissolved Hg concentration is due to adsorption by colloids formed at high E_h. In addition, demethylation of MeHg by bacteria (*Clostridium* spp.) contributed to MeHg decreasing. Our findings substantially improve the general understanding of the global biogeochemical cycle of Hg in the nature, particularly in frequently flooded zones of the entire world.

We highlighted (1) the importance of the largely overlooked interactions between dissolved Hg and colloids that are prevalent in the environment. In addition to the alteration of the microbial community, redox change from anaerobic to aerobic forms a large amount of colloids, which can bind with Hg to increase its mobilization but decrease its availability for methylation. (2) Hg methylation might be more significant than its demethylation in determining MeHg concentration during redox changes. We observed a clear decrease in the relative abundance of Hg demethylation bacteria with E_h increasing (Figure 5) and thus expected a weakened demethylation effect. In other words, the MeHg concentration reduction was weak. However, the MeHg concentration still decreased constantly with E_h rising (Figure 6A). We attributed this phenomenon to a significant decrease in MeHg formation, leading to a poor supplement of MeHg in the soil.

In a global context of increased demands for rice caused by population boom and persistent contamination of Hg in paddy soils, our results provide new insights into how MeHg can be formed and diminished and the degree of these effects, with the change in redox potential. Further, our results should be helpful for the design of a more effective management of Hg-contaminated soils worldwide. Here, we found that the increase in E_h by flushing with air or oxygen reduced the concentration of MeHg and bioavailable Hg in the soil. This may mitigate the risk of the transfer of Hg into rice and thus the exposure of MeHg via food consumption in highly Hg-contaminated areas. Therefore, periodic draining or aeration of paddy soils to increase the E_h provides a method that is less destructive and free of secondary contamination with a low energy consumption to control the risks of MeHg in soils of the world.

■ ASSOCIATED CONTENT

Supporting Information

The Supporting Information is available free of charge at https://pubs.acs.org/doi/10.1021/acs.est.0c07321.

More details about the methodology, including characterization of the studied soil, sample analysis, iron K-edge XANES spectroscopy analysis, STEM-EDX spectroscopy analysis, microorganism composition analysis, data-quality control, discussion on redox-dependent change of the relative abundance of microbial community, calculation of dissolved Hg concentrations in soil suspensions, table for relative abundances (%) of dominant OTU at the class level in overall microorganism communities and in the bulk soil and soils collected at different E_h conditions, figures showing the distribution of paddy fields in different regions in the world, X-ray diffraction (XRD) pattern of the studied soil, the relationship between dissolved Hg and dissolved Fe in the soil liquid phase across the E_h range of the study, Fe EXAFS K_2-weighted spectrum of the soil collected at different E_h conditions, photos of the colloids separated from the soil liquid phase, scanning transmission electron microscope (STEM) images of the colloidal particles, relationship between dissolved Hg and DOC in the soil liquid phase (<0.45 μM) for the redox range of the study, impact of predefined E_h conditions on sulfate concentration and chloride concentration in the soil liquid phase, relative abundances (%) of dominant OTU at the genus level in overall microorganism communities, relationship between the relative abundance of the studied bacteria and methylation potential (MeHg/THg) in the soil, relationship between the DOC-to-THg ratio and methylation potential (MeHg/THg) in the soil, relationship between the chloride and methylation potential (MeHg/THg) in the soil (PDF)

■ AUTHOR INFORMATION

Corresponding Author

Jörg Rinklebe − *Laboratory of Soil- and Groundwater-Management, Institute of Foundation Engineering, Water- and Waste-Management, School of Architecture and Civil Engineering, University of Wuppertal, 42285 Wuppertal, Germany; Department of Environment, Energy and Geoinformatics, University of Sejong, Seoul 05006, Republic of Korea;* orcid.org/0000-0001-7404-1639; Email: rinklebe@uni-wuppertal.de

Authors

Jianxu Wang − *State Key Laboratory of Environmental Geochemistry, Institute of Geochemistry, Chinese Academy of Sciences, Guiyang 550082, P. R. China; Laboratory of Soil- and Groundwater-Management, Institute of Foundation Engineering, Water- and Waste-Management, School of Architecture and Civil Engineering, University of Wuppertal, 42285 Wuppertal, Germany; CAS Center for Excellence in*

Quaternary Science and Global Change, Xi'an 710061, P. R. China; orcid.org/0000-0001-9198-0144

Sabry M. Shaheen − *Laboratory of Soil- and Groundwater-Management, Institute of Foundation Engineering, Water- and Waste-Management, School of Architecture and Civil Engineering, University of Wuppertal, 42285 Wuppertal, Germany; Department of Arid Land Agriculture, Faculty of Meteorology, Environment, and Arid Land Agriculture, King Abdulaziz University, Jeddah 21589, Kingdom of Saudi Arabia; Department of Soil and Water Sciences, Faculty of Agriculture, University of Kafrelsheikh, 33516 Kafr El-Sheikh, Egypt*

Min Jing − *State Key Laboratory of Environmental Geochemistry, Institute of Geochemistry, Chinese Academy of Sciences, Guiyang 550082, P. R. China*

Christopher W. N. Anderson − *Environmental Sciences, School of Agriculture and Environment, Massey University, 4442 Palmerston North, New Zealand*

Ann-Christin Swertz − *Department of Safety Technology and Environmental Protection, Faculty of Mechanical Engineering and Safety Engineering, University of Wuppertal, 42119 Wuppertal, Germany*

Shan-Li Wang − *Department of Agricultural Chemistry, National Taiwan University, Taipei 106, Taiwan, Republic of China;* orcid.org/0000-0003-3156-5365

Xinbin Feng − *State Key Laboratory of Environmental Geochemistry, Institute of Geochemistry, Chinese Academy of Sciences, Guiyang 550082, P. R. China; CAS Center for Excellence in Quaternary Science and Global Change, Xi'an 710061, P. R. China;* orcid.org/0000-0002-7462-8998

Complete contact information is available at: https://pubs.acs.org/10.1021/acs.est.0c07321

Notes

The authors declare no competing financial interest.

■ ACKNOWLEDGMENTS

The authors thank the German Alexander von Humboldt Foundation (Ref 3.5-1186537-CHN-HFST-P), the National Natural Science Foundation of China (42073081, 41931297, and 41573082), the Fundamental Research Program of Department of Science and Technology of Guizhou (ZK[2021]-key-045), and the Pioneer Hundred-Talent Program of Chinese Academy of Sciences for financial support. Many thanks to Beamline 07C at the National Synchrotron Radiation Research Center (NSRRC), ROC, for supporting Fe XANES analysis.

■ REFERENCES

(1) Beckers, F.; Rinklebe, J. Cycling of mercury in the environment: Sources, fate, and human health implications: A review. *Crit. Rev. Environ. Sci. Technol.* **2017**, *47*, 693−794.

(2) Liu, M.; Zhang, Q.; Cheng, M.; He, Y.; Chen, L.; Zhang, H.; Cao, H.; Shen, H.; Zhang, W.; Tao, S.; Wang, X. Rice life cycle-based global mercury biotransport and human methylmercury exposure. *Nat. Commun.* **2019**, *10*, No. 5164.

(3) Wang, J.; Xing, Y.; Xie, Y.; Meng, Y.; Xia, J.; Feng, X. The use of calcium carbonate-enriched clay minerals and diammonium phosphate as novel immobilization agents for mercury remediation: Spectral investigations and field applications. *Sci. Total Environ.* **2019**, *646*, 1615−1623.

(4) Man, Y.; Wang, B.; Wang, J.; Slaný, M.; Yan, H.; Li, P.; El-Naggar, A.; Shaheen, S. M.; Rinklebe, J.; Feng, X. Use of biochar to reduce mercury accumulation in *Oryza sativa* L.: A trial for sustainable management of historically polluted farmlands. *Environ. Int.* **2021**, *153*, No. 106527.

(5) Zhao, F. J.; Ma, Y. B.; Zhu, Y. G.; Tang, Z.; McGrath, S. P. Soil Contamination in China: Current Status and Mitigation Strategies. *Environ. Sci. Technol.* **2015**, *49*, 750−759.

(6) USGS. *Mineral Resources Data System*; US Geological Survey: Reston, VA, 2005.

(7) Li, X.; Zhang, J.; Gong, Y.; Yang, S.; Ye, M.; Yu, X.; Ma, J. Status of mercury accumulation in agricultural soils across China (1976−2016). *Ecotoxicol. Environ. Saf.* **2020**, *197*, No. 110564.

(8) O'Connor, D.; Hou, D.; Ok, Y. S.; Mulder, J.; Duan, L.; Wu, Q.; Wang, S.; Tack, F. M. G.; Rinklebe, J. Mercury speciation, transformation, and transportation in soils, atmospheric flux, and implications for risk management: A critical review. *Environ. Int.* **2019**, *126*, 747−761.

(9) Jonsson, S.; Skyllberg, U.; Nilsson, M. B.; Lundberg, E.; Andersson, A.; Björn, E. Differentiated availability of geochemical mercury pools controls methylmercury levels in estuarine sediment and biota. *Nat. Commun.* **2014**, *5*, No. 4624.

(10) Parks, J. M.; Johs, A.; Podar, M.; Bridou, R.; Hurt, R. A.; Smith, S. D.; Tomanicek, S. J.; Qian, Y.; Brown, S. D.; Brandt, C. C.; Palumbo, A. V.; Smith, J. C.; Wall, J. D.; Elias, D. A.; Liang, L. The Genetic Basis for Bacterial Mercury Methylation. *Science* **2013**, *339*, 1332−1335.

(11) Zhao, L.; Chen, H.; Lu, X.; Lin, H.; Christensen, G. K.; Pierce, E. M.; Gu, B. Contrasting Effects of Dissolved Organic Matter on Mercury Methylation by *Geobacter sulfurreducens* PCA and Desulfovibrio desulfuricans ND132. *Environ. Sci. Technol.* **2017**, *51*, 10468−10475.

(12) Zheng, W.; Demers, J. D.; Lu, X.; Bergquist, B. A.; Anbar, A. D.; Blum, J. D.; Gu, B. H. Mercury Stable Isotope Fractionation during Abiotic Dark Oxidation in the Presence of Thiols and Natural Organic Matter. *Environ. Sci. Technol.* **2019**, *53*, 1853−1862.

(13) Wang, X.; Ye, Z. H.; Li, B.; Huang, L. N.; Meng, M.; Shi, J. B.; Jiang, G. B. Growing Rice Aerobically Markedly Decreases Mercury Accumulation by Reducing Both Hg Bioavailability and the Production of MeHg. *Environ. Sci. Technol.* **2014**, *48*, 1878−1885.

(14) Ji, X. N.; Liu, C. B.; Zhang, M. Y.; Yin, Y. G.; Pan, G. Mitigation of methylmercury production in eutrophic waters by interfacial oxygen nanobubbles. *Water Res.* **2020**, *173*, No. 115563.

(15) Ramesh Reddy, K.; DeLaune, R. D. *Biogeochemistry of Wetlands: Science and Applications*; CRC Press, 2008.

(16) Shaheen, S. M.; Rinklebe, J.; Frohne, T.; White, J. R.; DeLaune, R. D. Biogeochemical Factors Governing Cobalt, Nickel, Selenium, and Vanadium Dynamics in Periodically Flooded Egyptian North Nile Delta Rice Soils. *Soil Sci. Soc. Am. J.* **2014**, *78*, 1065−1078.

(17) Cypionka, H. Sulfate-Reducing Bacteria. In *Encyclopedia of Geobiology*; Reitner, J.; Thiel, V., Eds.; Springer Netherlands: Dordrecht, 2011; pp 853−855.

(18) Drott, A.; Lambertsson, L.; Björn, E.; Skyllberg, U. Importance of Dissolved Neutral Mercury Sulfides for Methyl Mercury Production in Contaminated Sediments. *Environ. Sci. Technol.* **2007**, *41*, 2270−2276.

(19) Benoit, J. M.; Gilmour, C. C.; Mason, R. P.; Heyes, A. Sulfide Controls on Mercury Speciation and Bioavailability to Methylating Bacteria in Sediment Pore Waters. *Environ. Sci. Technol.* **1999**, *33*, 951−957.

(20) Trivedi, P.; Axe, L. Predicting divalent metal sorption to hydrous Al, Fe, and Mn oxides. *Environ. Sci. Technol.* **2001**, *35*, 1779−1784.

(21) Tiffreau, C.; Lützenkirchen, J.; Behra, P. Modeling the Adsorption of Mercury(II) on (Hydr)oxides: I. Amorphous Iron Oxide and α-Quartz. *J. Colloid Interface Sci.* **1995**, *172*, 82−93.

(22) Korehi, H.; Blöthe, M.; Sitnikova, M. A.; Dold, B.; Schippers, A. Metal Mobilization by Iron- and Sulfur-Oxidizing Bacteria in a Multiple Extreme Mine Tailings in the Atacama Desert, Chile. *Environ. Sci. Technol.* **2013**, *47*, 2189−2196.

(23) John, D. A.; Leventhal, J. S. *Bioavailability of Metals. Preliminary Compilation of Descriptive Geoenvironmental Mineral Deposit Models*; 1995; pp 10−18.
(24) DIN EN 15935: Schlamm, behandelter Bioabfall Boden und Abfall-Bestimmung des Glühverlusts, 2012.
(25) Yu, K.; Rinklebe, J. Advancement in soil microcosm apparatus for biogeochemical research. *Ecol. Eng.* **2011**, *37*, 2071−2075.
(26) Rinklebe, J.; Shaheen, S. M.; Schröter, F.; Rennert, T. Exploiting biogeochemical and spectroscopic techniques to assess the geochemical distribution and release dynamics of chromium and lead in a contaminated floodplain soil. *Chemosphere* **2016**, *150*, 390−397.
(27) Hall, G. E. M.; Pelchat, J. C.; Pelchat, P.; Vaive, J. E. Sample collection, filtration and preservation protocols for the determination of 'total dissolved' mercury in waters. *Analyst* **2002**, *127*, 674−680.
(28) Rinklebe, J.; Shaheen, S. M.; El-Naggar, A.; Wang, H.; Du Laing, G.; Alessi, D. S.; Ok, Y. S. Redox-induced mobilization of Ag, Sb, Sn, and Tl in the dissolved, colloidal and solid phase of a biochar-treated and un-treated mining soil. *Environ. Int.* **2020**, *140*, No. 105754.
(29) Wang, J.; Shaheen, S. M.; Swertz, A.-C.; Rennert, T.; Feng, X.; Rinklebe, J. Sulfur-modified organoclay promotes plant uptake and affects geochemical fractionation of mercury in a polluted floodplain soil. *J. Hazard. Mater.* **2019**, *371*, 687−693.
(30) USEPA. *Method 1630: Methyl Mercury in Water by Distillation, Aqueous Ethylation, Purge and Trap, and CVAFS*, 2001.
(31) Ren, G.; Zhang, H.; Lin, X.; Zhu, J.; Jia, Z. Response of phyllosphere bacterial communities to elevated CO_2 during rice growing season. *Appl. Microbiol. Biotechnol.* **2014**, *98*, 9459−9471.
(32) de Castro, A. F.; Ehrlich, H. L. Reduction of iron oxide minerals by a marine Bacillus. *Antonie van Leeuwenhoek* **1970**, *36*, 317−327.
(33) Suter, D.; Banwart, S.; Stumm, W. Dissolution of hydrous iron(III) oxides by reductive mechanisms. *Langmuir* **1991**, *7*, 809−813.
(34) Ionescu, D.; Heim, C.; Polerecky, L.; Thiel, V.; de Beer, D. Biotic and abiotic oxidation and reduction of iron at circumneutral pH are inseparable processes under natural conditions. *Geomicrobiol. J.* **2015**, *32*, 221−230.
(35) Weber, F.-A.; Voegelin, A.; Kaegi, R.; Kretzschmar, R. Contaminant mobilization by metallic copper and metal sulphide colloids in flooded soil. *Nat. Geosci.* **2009**, *2*, 267.
(36) Ghorishi, S. B.; Sedman, C. B. Low Concentration Mercury Sorption Mechanisms and Control by Calcium-Based Sorbents: Application in Coal-Fired Processes. *J. Air Waste Manage. Assoc.* **1998**, *48*, 1191−1198.
(37) Wang, Y.; Huo, Q.; Shi, L.; Feng, G.; Wang, J.; Han, L.; Chang, L. Adsorption of mercury species on selected CuS surfaces and the effects of HCl. *Chem. Eng. J.* **2020**, *393*, No. 124773.
(38) Pavlin, M.; Popović, A.; Jaćimović, R.; Horvat, M. Mercury fractionation in gypsum using temperature desorption and mass spectrometric detection. *Open Chem.* **2018**, *16*, 544−555.
(39) Inoue, K.; Aomine, K. Retention of mercury by soil colloids. *Soil Sci. Plant Nutr.* **1969**, *15*, 86−91.
(40) Slowey, A. J.; Johnson, S. B.; Rytuba, J. J.; Brown, G. E. Role of Organic Acids in Promoting Colloidal Transport of Mercury from Mine Tailings. *Environ. Sci. Technol.* **2005**, *39*, 7869−7874.
(41) Jin, Z.; Shah, T.; Zhang, L.; Liu, H.; Peng, S.; Nie, L. Effect of straw returning on soil organic carbon in rice−wheat rotation system: A review. *Food Energy Secur.* **2020**, *9*, No. e200.
(42) Jokinen, H. K.; Kiikkilä, O.; Fritze, H. Exploring the mechanisms behind elevated microbial activity after wood ash application. *Soil Biol. Biochem.* **2006**, *38*, 2285−2291.
(43) Yu, K.; Böhme, F.; Rinklebe, J.; Neue, H.-U.; DeLaune, R. D. Major biogeochemical processes in soils-A microcosm incubation from reducing to oxidizing conditions. *Soil Sci. Soc. Am. J.* **2007**, *71*, 1406−1417.
(44) LeMonte, J. J.; Stuckey, J. W.; Sanchez, J. Z.; Tappero, R.; Rinklebe, Jr.; Sparks, D. L. Sea level rise induced arsenic release from historically contaminated coastal soils. *Environ. Sci. Technol.* **2017**, *51*, 5913−5922.
(45) Sparks, D. L. *Environmental Soil Chemistry*; Elsevier, 2003.
(46) Gilmour, C. C.; Podar, M.; Bullock, A. L.; Graham, A. M.; Brown, S. D.; Somenahally, A. C.; Johs, A.; Hurt, R. A.; Bailey, K. L.; Elias, D. A. Mercury Methylation by Novel Microorganisms from New Environments. *Environ. Sci. Technol.* **2013**, *47*, 11810−11820.
(47) Zhou, X.-Q.; Hao, Y.-Y.; Gu, B.; Feng, J.; Liu, Y.-R.; Huang, Q. Microbial Communities Associated with Methylmercury Degradation in Paddy Soils. *Environ. Sci. Technol.* **2020**, *54*, 7952−7960.
(48) Skyllberg, U.; Drott, A.; Lambertsson, L.; Björn, E.; Karlsson, T.; Johnson, T.; Heinemo, S.-Å.; Holmström, H. Net methylmercury production as a basis for improved risk assessment of mercury-contaminated sediments. *Ambio* **2007**, *36*, 437−443.
(49) Shanley, J. B.; Kamman, N. C.; Clair, T. A.; Chalmers, A. Physical Controls on Total and Methylmercury Concentrations in Streams and Lakes of the Northeastern USA. *Ecotoxicology* **2005**, *14*, 125−134.
(50) Paranjape, A. R.; Hall, B. D. Recent advances in the study of mercury methylation in aquatic systems. *FACETS* **2017**, *2*, 85−119.
(51) Bravo, A. G.; Cosio, C. Biotic formation of methylmercury: A bio−physico−chemical conundrum. *Limnol. Oceanogr.* **2020**, *65*, 1010−1027.
(52) Liu, J.; Wang, J.; Ning, Y.; Yang, S.; Wang, P.; Shaheen, S. M.; Feng, X.; Rinklebe, J. Methylmercury production in a paddy soil and its uptake by rice plants as affected by different geochemical mercury pools. *Environ. Int.* **2019**, *129*, 461−469.
(53) Celo, V.; Lean, D. R. S.; Scott, S. L. Abiotic methylation of mercury in the aquatic environment. *Sci. Total Environ.* **2006**, *368*, 126−137.
(54) Zhang, H.; Feng, X.; Larssen, T.; Shang, L.; Vogt, R. D.; Lin, Y.; Li, P.; Zhang, H. Fractionation, distribution and transport of mercury in rivers and tributaries around Wanshan Hg mining district, Guizhou Province, Southwestern China: Part 2 − Methylmercury. *Appl. Geochem.* **2010**, *25*, 642−649.
(55) Hammerschmidt, C. R.; Fitzgerald, W. F. Photodecomposition of Methylmercury in an Arctic Alaskan Lake. *Environ. Sci. Technol.* **2006**, *40*, 1212−1216.
(56) Frohne, T.; Rinklebe, J.; Langer, U.; Du Laing, G.; Mothes, S.; Wennrich, R. Biogeochemical factors affecting mercury methylation rate in two contaminated floodplain soils. *Biogeosciences* **2012**, *9*, 493−507.
(57) Bravo, A. G.; Bouchet, S.; Tolu, J.; Björn, E.; Mateos-Rivera, A.; Bertilsson, S. Molecular composition of organic matter controls methylmercury formation in boreal lakes. *Nat. Commun.* **2017**, *8*, No. 14255.
(58) Moreau, J. W.; Gionfriddo, C. M.; Krabbenhoft, D. P.; Ogorek, J. M.; DeWild, J. F.; Aiken, G. R.; Roden, E. E. The Effect of Natural Organic Matter on Mercury Methylation by *Desulfobulbus propionicus* 1pr3. *Front. Microbiol.* **2015**, *6*, No. 1389.
(59) Jiménez-Moreno, M.; Perrot, V.; Epov, V. N.; Monperrus, M.; Amouroux, D. Chemical kinetic isotope fractionation of mercury during abiotic methylation of Hg(II) by methylcobalamin in aqueous chloride media. *Chem. Geol.* **2013**, *336*, 26−36.

https://doi.org/10.1021/acs.est.0c07321
Environ. Sci. Technol. 2021, 55, 10133−10141